UROGENITAL

Evaluation of a fractional-order calculus diffusion model and bi-parametric VI-RADS for staging and grading bladder urothelial carcinoma

Cui Feng[1,2] · Yanchun Wang[1] · Guangyu Dan[2,3] · Zheng Zhong[2,3] · M. Muge Karaman[2,3] · Zhen Li[1] · Daoyu Hu[1] · Xiaohong Joe Zhou[2,3,4,5]

Abstract

Objectives To evaluate the feasibility of high b-value diffusion-weighted imaging (DWI) for distinguishing non-muscle-invasive bladder cancer (NMIBC) from muscle-invasive bladder cancer (MIBC) and low- from high-grade bladder urothelial carcinoma using a fractional-order calculus (FROC) model as well as a combination of FROC DWI and bi-parametric Vesical Imaging-Reporting and Data System (VI-RADS).

Methods Fifty-eight participants with bladder urothelial carcinoma were included in this IRB-approved prospective study. Diffusion-weighted images, acquired with 16 b-values (0–3600 s/mm^2), were analyzed using the FROC model. Three FROC parameters, D, β, and μ, were used for delineating NMIBC from MIBC and for tumor grading. A receiver operating characteristic (ROC) analysis was performed based on the individual FROC parameters and their combinations, followed by comparisons with apparent diffusion coefficient (ADC) and bi-parametric VI-RADS based on T2-weighted images and DWI.

Results D and μ were significantly lower in the MIBC group than in the NMIBC group ($p = 0.001$ for each), and D, β, and μ all exhibited significantly lower values in the high- than in the low-grade tumors ($p \leq 0.011$). The combination of D, β, and μ produced the highest specificity (85%), accuracy (78%), and the area under the ROC curve (AUC, 0.782) for distinguishing NMIBC and MIBC, and the best sensitivity (89%), specificity (86%), accuracy (88%), and AUC (0.892) for tumor grading, all of which outperformed the ADC. The combination of FROC parameters with bi-parametric VI-RADS improved the AUC from 0.859 to 0.931.

Conclusions High b-value DWI with a FROC model is useful in distinguishing NMIBC from MIBC and grading bladder tumors.

Key Points
• *Diffusion parameters derived from a FROC diffusion model may differentiate NMIBC from MIBC and low- from high-grade bladder urothelial carcinomas.*
• *Under the condition of a moderate sample size, higher AUCs were achieved by the FROC parameters D (0.842) and μ (0.857) than ADC (0.804) for bladder tumor grading with p ≤ 0.046.*
• *The combination of the three diffusion parameters from the FROC model can improve the specificity over ADC (85% versus 67%, p = 0.031) for distinguishing NMIBC and MIBC and enhance the performance of bi-parametric VI-RADS.*

Keywords Urinary bladder neoplasms · Diffusion magnetic resonance imaging · Neoplasm grading

Drs. Xiaohong Joe Zhou and Daoyu Hu are the senior authors who share the co-corresponding authorship.

✉ Daoyu Hu
daoyuhu@hust.edu.cn

✉ Xiaohong Joe Zhou
xjzhou@uic.edu

[1] Department of Radiology, Tongji Hospital, Tongji Medical College, Huazhong University of Science and Technology, 1095 Jiefang Avenue, Qiaokou District, Wuhan 430030, China

[2] Center for MR Research, University of Illinois at Chicago, MC-707, Suite 1A, 1801 West Taylor Street, Chicago, IL 60612, USA

[3] Department of Bioengineering, University of Illinois at Chicago, Chicago, IL, USA

[4] Department of Radiology, University of Illinois at Chicago, Chicago, IL, USA

[5] Department of Neurosurgery, University of Illinois at Chicago, Chicago, IL, USA

Abbreviations

ADC   Apparent diffusion coefficient
AUC   Area under the curve
BC   Bladder cancer
DCE   Dynamic contrast-enhanced
DWI   Diffusion-weighted imaging
FOV   Field of view
FROC   Fractional-order calculus
FSE   Fast spin-echo
MIBC   Muscle-invasive bladder cancer
NMIBC   Non-muscle-invasive bladder cancer
ROC   Receiver operating characteristic
TURBT   Transurethral resection of bladder tumor
VI-RADS   Vesical Imaging Reporting and Data System

Introduction

Bladder cancer is the tenth most common cancer worldwide, with 549,000 new cases and approximately 200,000 deaths in 2018 [1]. The majority of bladder cancer is histologically classified as urothelial carcinoma whose management strategy is determined mainly based on the depth of invasion and histologic grade [2, 3]. For patients with non-muscle-invasive bladder cancer (NMIBC; stage T1 or lower), transurethral resection of bladder tumor (TURBT) is typically recommended [2], while more aggressive muscle-invasive bladder cancers (MIBC; stage T2 or higher) frequently require radical cystectomy, adjuvant chemotherapy, or both [3]. Accurate assessment of the presence or absence of muscular invasion and the degree of tumor cell differentiation is essential not only for selecting the best treatment options but also for sparing patients with low-risk NMIBC from unnecessary invasive treatment.

Clinically, TURBT is a standard method to determine muscle-invasiveness and histologic grade [2, 3]. It was reported, however, that tumors can be under-staged in up to 25% of muscle-invasive bladder cancers, and inaccurate grading occurs in up to 15% of tumors due to sampling errors [4, 5]. These limitations, as well as the high cost and invasiveness of TURBT procedures, indicate that a noninvasive and a more accurate imaging technique is highly desirable to assist in staging and/or grading bladder urothelial carcinomas.

Diffusion-weighted imaging (DWI) can reveal tissue microstructural alterations *in vivo*, particularly in cancer [6, 7]. Among many quantitative parameters that DWI offers, apparent diffusion coefficient (ADC) has been increasingly used for characterizing bladder urothelial carcinoma [8–11], as evidenced by the recently developed Vesical Imaging-Reporting and Data System (VI-RADS) [12, 13]. Considering the varying degrees of structural complexity in cancer tissues, sophisticated non-Gaussian diffusion models [14, 15] may provide a more comprehensive characterization of bladder urothelial carcinoma. Among these, a fractional-order calculus (FROC) model [16] is of particular interest because it has been found useful for grading pediatric brain tumors [17, 18], correlating with Lauren classification in gastric cancer [19], and assessing treatment response of gastrointestinal stroma tumors [20]. The FROC model offers three parameters: diffusion coefficient D (in μm^2/ms), fractional-order derivative in space β (dimensionless), and a spatial parameter μ (in μm). These parameters, individually or conjointly, can provide a multi-faceted characterization of tissues based on not only cellularity but also structural heterogeneity. When combined with VI-RADS, they may also enhance the diagnostic performance. In this study, we investigated the feasibility of using DWI with the FROC model at high b-values for staging and grading urothelial carcinoma, compared the performance of FROC parameters with that of ADC, and investigated the possible improvement in diagnostic performance when the FROC parameters are combined with a simplified version of VI-RADS.

Materials and methods

Patient characteristics

This prospective study was approved by the Institutional Review Board of Tongji Hospital, and written informed consent was obtained from all participants. Eighty-seven patients with suspected or confirmed bladder lesions (e.g., by ultrasonography or CT) were enrolled and underwent MRI between July 2014 and August 2019. Additional inclusion criteria were (i) no therapy performed on the newly suspected or detected lesions prior to the MRI examination and (ii) no contraindications to MRI (e.g., claustrophobia, metal objects in or on the body). The exclusion criteria consisted of (i) unavailability of histopathological confirmation through TURBT or cystectomy after the MRI examination ($n = 8$), (ii) confirmed non-urothelial carcinoma ($n = 17$), (iii) poor image quality due to excessive motion artifacts ($n = 1$), or (iv) insufficient tumor area (less than 50 mm^2) for reliably placing regions of interest (ROIs) ($n = 3$). With these criteria, a total of fifty-eight participants (51 men and 7 women; mean age = 60 ± 10 years; age range = 37–79 years) were included in the analysis. Two out of the fifty-eight participants had recurrent tumors. However, the time relapsed between the previous treatment and the MRI examination of the recurrent tumors was 1 and 9 years, respectively. Hence, the prior treatment was not expected to affect the MRI scans as supported by the literature [12]. After the MRI examination, patients underwent TURBT alone, TURBT followed by partial or radical cystectomy, or cystectomy directly. TURBT was performed within 1 to 22 days (mean, 4 days) of the MRI examination, and direct
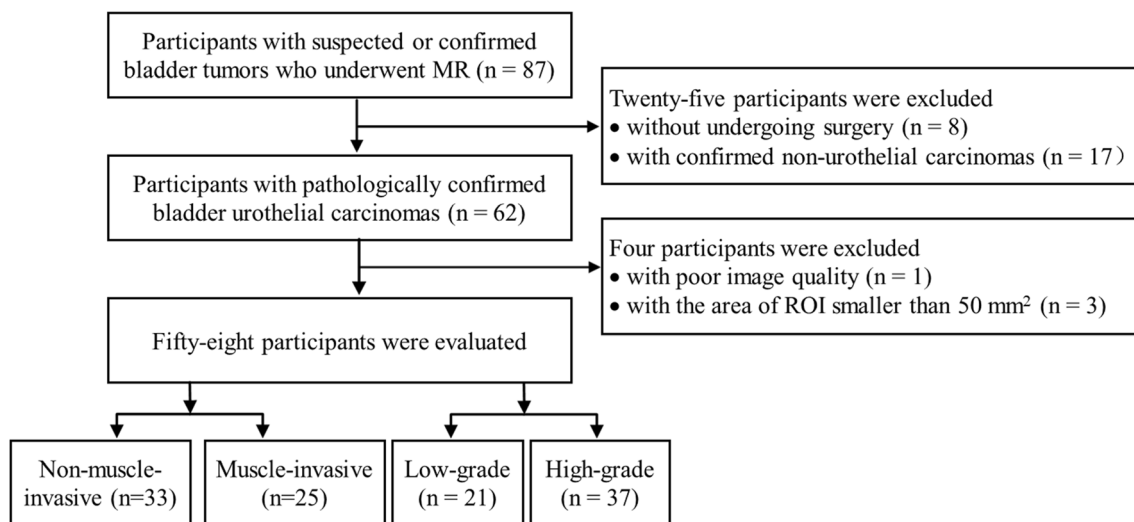
Fig. 1 Flowchart of the study population

cystectomy within 2 weeks (mean, 7 days). For the patients who underwent cystectomy after TURBT, the interval between the two procedures was typically less than one week. A flowchart of the study population is given in Fig. 1.

Image acquisition

All participants underwent MR examinations on a 3-T scanner (Discovery MR750; GE Healthcare) in the supine position with a 32-channel torso phased-array coil. The imaging protocol included axial fast spin-echo (FSE) T1-weighted, axial fast-recovery FSE T2-weighted, sagittal FSE T2-weighted, and multi-b-value diffusion-weighted sequences. The acquisition parameters of each non-diffusion imaging sequence were as follows: (i) axial T1-weighted imaging: repetition time (TR)/echo time (TE) = 528/6.8 ms, field of view = 340 × 340 mm^2, matrix size = 320 × 256, and echo train length = 4; (ii) axial fast recovery T2-weighted imaging: TR/TE = 3780/75 ms, field of view = 340 × 340 mm^2, matrix size = 320 × 256, and echo train length = 16; (iii) sagittal T2-weighted imaging: TR/TE = 5500/75 ms, field of view = 240 × 240 mm^2, matrix size = 320 × 320, and echo train length = 24. In all sequences above, a slice thickness of 4 mm with an inter-slice gap of 1 mm was used with 2 averages. A series of axial diffusion-weighted images were acquired using a single-shot spin-echo echo-planar imaging sequence with 16 b-values: 0_1, 50_1, 80_1, 100_1, 150_1, 200_1, 300_2, 500_2, 800_2, 1000_4, 1300_4, 1700_6, 1800_6, 2400_6, 3000_8, and 3600_{10} s/mm^2, where the subscript denotes the number of averages. At each non-zero b-value, a Stejskal-Tanner diffusion gradient was successively applied along the three orthogonal directions to obtain trace-weighted images to mitigate the influence of diffusion anisotropy. The other acquisition parameters for the DWI sequence were: TR/TE = 2500/84 ms, field of view = 400 × 400 mm^2, matrix size = 128 × 160, slice thickness = 4

mm, inter-slice gap = 1 mm, separation between the Stejskal-Tanner gradient lobes (Δ) = 43.56 ms, duration of each diffusion gradient lobe (δ) = 32.20 ms, and the scan time = 6–8 minutes depending on the number of slices to fully cover the anatomy.

Image analysis

In the FROC model, the diffusion-weighted signal S is expressed as:

$$S = S_0 \exp\left[-D\mu^{2(\beta-1)}(\gamma G_d \delta)^{2\beta}\left(\Delta - \frac{2\beta-1}{2\beta+1}\delta\right)\right] \quad (1)$$

where S_0 is the signal intensity without diffusion weighting, G_d is the diffusion gradient amplitude, Δ and δ are the Stejskal-Tanner diffusion gradient parameters defined above, D (in units of μm^2/ms) is the anomalous diffusion coefficient similar to ADC, β (dimensionless) is a spatial fractional-order index that has been linked to intra-voxel tissue heterogeneity, and μ (in units of μm) is a spatial parameter related to tissue microstructures, as further explained in reference [16]. Based on Eq. (1), the three FROC parameter maps (D, β, and μ) were generated voxel-by-voxel by fitting the FROC model to the diffusion images acquired with the 16 b-values using a Levenberg-Marquardt nonlinear fitting algorithm [16].

For comparison, the conventional ADC map was also obtained by employing a mono-exponential function to fit to the diffusion-weighted images. All fittings were performed using customized software developed in MATLAB (MathWorks, Inc).

For participants with multifocal lesions, only the tumor with the largest diameter was analyzed. For the selected tumor, region of interest (ROI) was manually drawn on the diffusion-weighted image with b = 1000 s/mm^2 for each

patient by two radiologists independently (C.F. and Y.C.W., with 11 and 7 years of experience in body MR diagnosis, respectively). The tumor stalk that exhibited lower signal intensity on diffusion-weighted images was excluded, as recommended by Kobayashi et al [8]. In addition, a minimum ROI threshold of 50 mm^2 was used to reduce the statistical bias, resulting in a median area of 181 mm^2 with a range of 54–3376 mm^2 among all participants.

VI-RADS scoring

Because dynamic contrast-enhanced (DCE) MRI was not available on the patients prior to the adoption of VI-RADS, a "bi-parametric VI-RADS" using T2-weighted and diffusion-weighted images was performed by two radiologists independently (C.F. and Y.C.W.) without the knowledge of histopathologic findings. Each selected tumor was scored with the 5-point scoring system, as described in previous studies [12, 21]. Bi-parametric VI-RADS scores from representative participants are shown in Fig. 2.

Statistical analysis

Statistical analysis was performed by using SPSS (Version 23.0) and MedCalc software (Version 18.9). For each participant, the mean value of each diffusion parameter (D, β, μ, and ADC) over the ROI was computed, followed by comparisons between the NMIBC and MIBC groups and between the low- and high-grade groups using a Mann-Whitney U-test, and a Bonferroni-Holm-adjusted significance level of $\alpha/4 = 0.0125$. The inter-observer reproducibility of ROI selection was evaluated by using a DICE index [22].

In addition to comparisons based on the individual parameters, different combinations of the FROC parameters (D, β, and μ) were also investigated by using a multivariate logistic regression, assuming that the possibility of being a high-grade or muscle-invasive tumor (P_0) follows a logistic model:

$$P_0 = \exp(a_0 + a_1 D + a_2 \beta + a_3 \mu)/[1 + \exp(a_0 + a_1 D + a_2 \beta + a_3 \mu)] \qquad (2)$$

where a_0 is a constant, and a_1, a_2, and a_3 are the regression coefficients for D, β, and μ, respectively [23]. Using Eq. (2), four combinations of the FROC parameters were investigated:
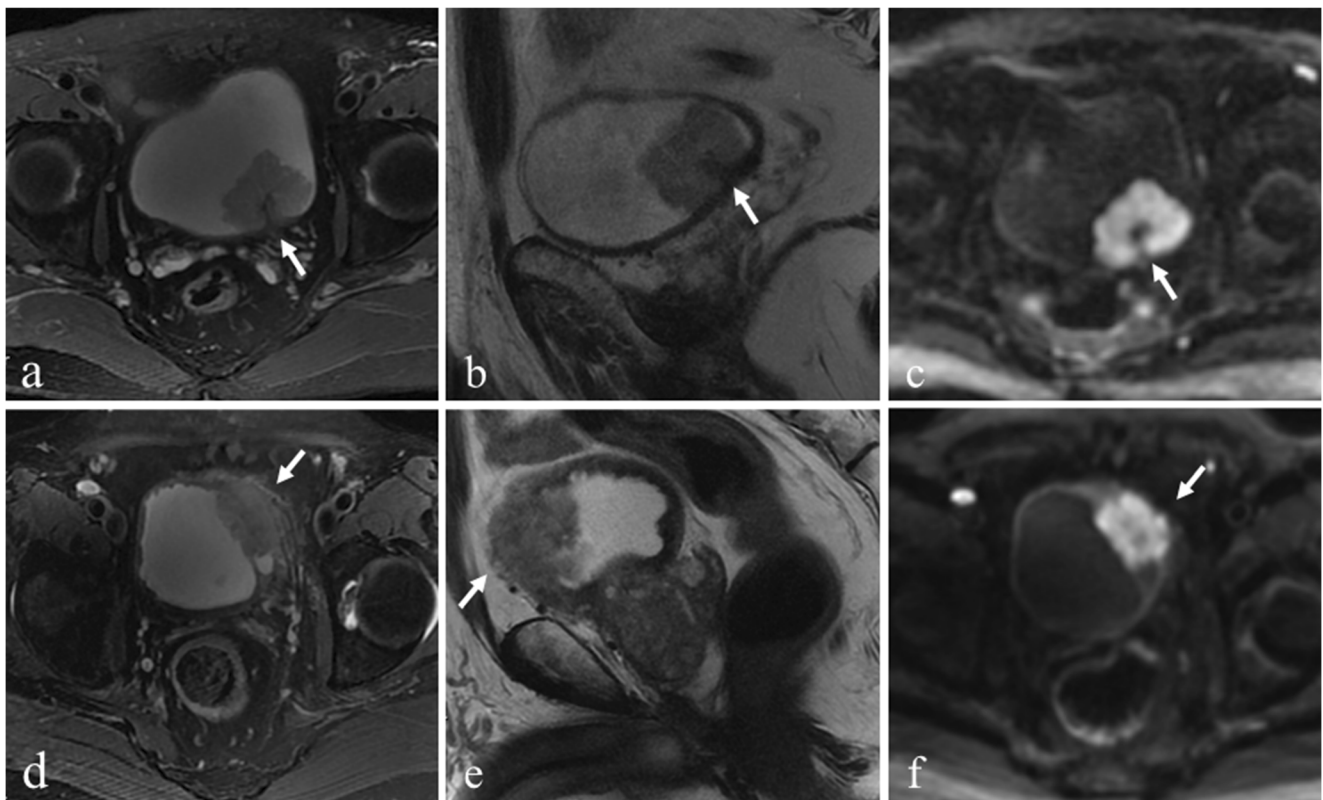

Fig. 2 *Upper row*: a patient with NMIBC. Axial (**a**) and sagittal (**b**) T2-weighted images illustrate an exophytic tumor on the left posterior wall with a low-signal-intensity stalk (arrows) and uninterrupted muscularis propria line, suggesting a T2-weighted imaging score of 2. A diffusion-weighted image (**c**) with $b = 1000$ s/mm^2 shows a high-signal-intensity tumor with a low-signal-intensity stalk (arrow), suggesting a DWI score of 2. A final bi-parametric VI-RADS score of 2 was determined. *Lower row*: a patient with MIBC. Axial (**d**) and sagittal (**e**) T2-weighted images illustrate a tumor on the left lateral wall with extension to extravesical fat (arrows), indicating a T2-weighted imaging score of 5. A diffusion-weighted image (**f**) with $b = 1000$ s/mm^2 shows high-signal-intensity tumor extending to the extravesical fat (arrow), suggesting a DWI score of 5. A final bi-parametric VI-RADS score of 5 was determined

(D, β), (β, μ), (D, μ), and (D, β, μ), by selectively nullifying the non-contributing regression coefficients in the two-parameter combinations.

For diffusion parameters individually or jointly, a receiver operating characteristic (ROC) analysis was performed to determine the best sensitivity, specificity, diagnostic accuracy, and the area under the ROC curve (AUC) with its 95% confidence interval (CI) for differentiating between the NMIBC and MIBC groups, and between the low- and high-grade tumor groups. The best cut-off sensitivity and specificity values of the ROC curves were determined by using the point closest to the upper left corner (i.e., sensitivity = 1, specificity = 1) in the ROC plot [24]. The sensitivity, specificity, and accuracy achieved by the individual FROC parameters and their combinations were compared with those by ADC by employing a McNemar test [25] for paired binomial responses, while their AUCs were compared by using a Hanley and McNeil test [26].

The inter-observer reliability of the bi-parametric VI-RADS ratings given by the two radiologists was evaluated by calculating the weighted kappa coefficient, followed by an ROC analysis to evaluate the diagnostic accuracy and AUC of bi-parametric VI-RADS. In addition, the three FROC parameters (D, β, μ) were combined with the bi-parametric VI-RADS results in another ROC analysis to assess the added value of the FROC parameters to bi-parametric VI-RADS.

Results

Clinical characteristics

The participants' clinical characteristics are summarized in Table 1. Among the 58 participants, 30 underwent TURBT, 1 TURBT followed by partial cystectomy, 3 TURBT followed by radical cystectomy, 3 partial cystectomy, and 21 radical cystectomy. The pathological T stage was determined according to the 2017 TNM system [27], yielding 10, 23, 16, 2, and 7 stage Ta, T1, T2, T3, and T4 tumors, respectively. Subsequently, 33 participants with stage Ta–T1 were classified into the NMIBC group and 25 participants with stages T2–T4 into the MIBC group [2]. The tumors were classified as low-grade in 21 participants and high-grade in 37 participants according to the 2016 World Health Organization classification system [28].

Diffusion imaging results from representative participants

Figure 3 displays a set of axial images from a representative patient with a low-grade NMIBC (top row) and another representative patient with a high-grade MIBC (bottom row). The columns show the T2-weighted images (Fig. 3 a and g), the

Table 1 Clinical characteristics

Variables	Characteristics
Age (years)[*]	60 ± 10 (37–79)
Gender	
Male	51 (87.9)
Female	7 (12.1)
No. of lesions	
Unifocal	43 (74.1)
Multifocal	15 (25.9)
Primary or recurrent tumors	
Primary	56 (96.6)
Recurrent	2 (3.4)
Tumor size (cm)[*]	3.1 ± 1.6 (1.0–10.1)
Pathologic stage	
Ta	10 (17.2)
T1	23 (39.7)
T2	16 (27.6)
T3	2 (3.4)
T4	7 (12.1)
Histologic grade	
Low	21 (36.2)
High	37 (63.8)
Lymph node metastasis	
Yes	11 (19.0)
No	47 (81.0)
Treatment methods	
TURBT	30 (51.7)
TURBT + partial cystectomy	1 (1.7)
TURBT + radical cystectomy	3 (5.2)
Partial cystectomy	3 (5.2)
Radical cystectomy	21 (36.2)

Numbers in parentheses are percentages except where otherwise indicated

TURBT, transurethral resection of bladder tumor

*Numbers are means ± standard deviations, with ranges in parentheses

diffusion-weighted images at b-value of 1000 s/mm^2 (Fig. 3 b and h), the FROC parameter maps (Fig. 3 c–e and i–k), and the ADC maps (Fig. 3 f and l). The D, β, μ, and ADC maps all exhibited higher values in the patient with low-grade NMIBC as compared to the patient with high-grade MIBC.

Comparison of diffusion parameters among different histopathologic subgroups

In the inter-observer reproducibility analysis, acceptable ROI selection consistency was achieved in all subjects with an overall DICE index of 0.89 ± 0.06 (mean ± standard deviation), in accordance with the literature [29]. Nearly 80% of
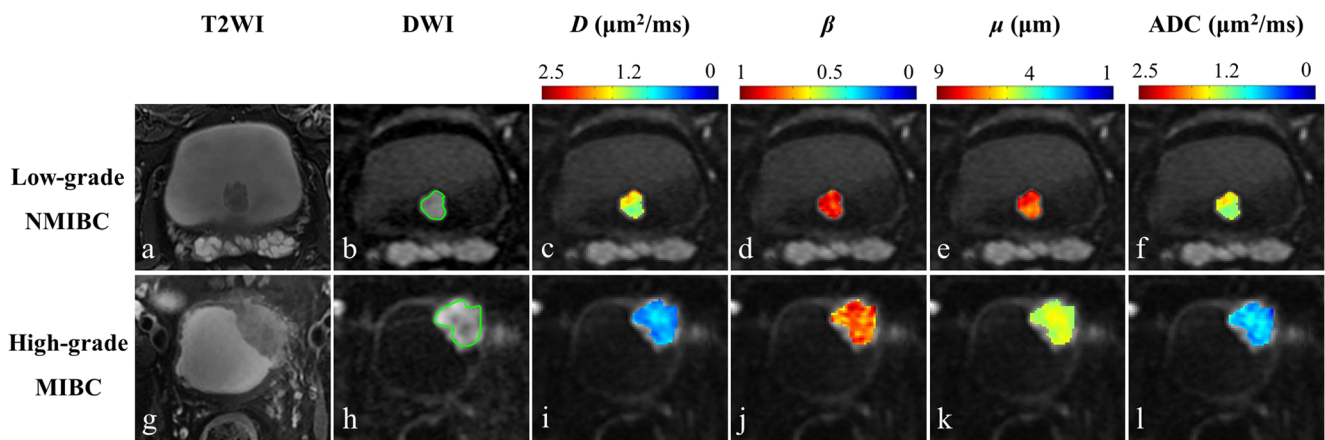
Fig. 3 Diffusion-weighted images and maps of the FROC parameters and ADC from a 64-year-old male with low-grade NMIBC (top row) and a 72-year-old male with high-grade MIBC (bottom row). The green contours in (**b**) and (**h**) indicate the tumor ROIs on the diffusion-weighted images with a b-value of 1000 s/mm^2. The remaining columns display T2-weighted images (**a**, **g**), the parameter maps of D (**c**, **i**), β (**d**, **j**), μ (**e**, **k**), and ADC (**f**, **l**) within the tumor ROIs. All three FROC parameters and ADC exhibited lower values in the high-grade MIBC (D: 0.86 μm^2/ms, β: 0.77, μ: 5.75 μm, and ADC: 0.95 μm^2/ms) than those in the low-grade NMIBC (D: 1.75 μm^2/ms, β: 0.86, μ: 8.16 μm, and ADC: 1.72 μm^2/ms)

DICE indices ranged from 0.83 to 0.95, demonstrating good performance.

The mean and standard deviation of each individual diffusion parameter for each patient group (i.e., the NMIBC, MIBC, low- and high-grade groups) are listed in Table 2. The values for D, μ, and ADC were significantly lower in the MIBC than those in the NMIBC group ($p = 0.001$, $p = 0.001$, and $p = 0.003$, respectively), whereas there were no significant differences in β between the two groups ($p = 0.126$). All parameters exhibited significantly lower values in the high- than in the low-grade urothelial carcinomas ($p < 0.001$ for D, μ, and ADC; $p = 0.011$ for β). The difference in FROC parameters and ADC are further illustrated in Fig. 4 as boxplots.

Performance of the diffusion parameters for tumor characterization

Table 3 summarizes the diagnostic performance of the FROC parameters and ADC for differentiating between the NMIBC and MIBC and between the low- and high-grade groups. The ROC curves of the diffusion parameters for delineating NMIBC from MIBC and low- from high-grade groups are shown in Fig. 5 a and b, respectively. Among the three FROC model parameters, D exhibited a similar diagnostic accuracy to μ for differentiating NMIBC from MIBC (D, 72%; μ, 74%) and for tumor grading (D, 79%; μ, 79%), both of which outperformed β. In addition, the AUCs of D (0.842) and μ (0.857) were significantly higher than that of ADC (0.804; $p \leq 0.046$) in discriminating low- from high-grade tumors.

The performance for tumor characterization was further analyzed by using combinations of the FROC parameters (Table 3). For delineating NMIBC from MIBC, (D, β) and (D, β, μ) offered identical diagnostic performance, both with significantly higher specificity (85%) than that of μ (67%, $p = 0.031$) or ADC (67%, $p = 0.031$). For delineating low- from high-grade tumors, all the four combinations improved the diagnostic performance when compared with individual FROC parameters, with the combination of all FROC parameters (D, β, μ) yielding the highest AUC (0.892), sensitivity

Table 2 Comparison of FROC parameters (D, β, and μ) and ADC among different histopathologic subgroups

	NMIBC ($n = 33$)	MIBC ($n = 25$)	p value	Low-grade ($n = 21$)	High-grade ($n = 37$)	p value
D (μm^2/ms)	1.24 ± 0.37	0.93 ± 0.27	0.001[*]	1.38 ± 0.31	0.96 ± 0.29	< 0.001[*]
β	0.76 ± 0.07	0.72 ± 0.05	0.126	0.78 ± 0.07	0.72 ± 0.05	0.011[*]
μ (μm)	6.94 ± 1.27	5.99 ± 0.75	0.001[*]	7.45 ± 1.17	6.01 ± 0.79	< 0.001[*]
ADC (μm^2/ms)	1.30 ± 0.31	1.06 ± 0.24	0.003[*]	1.40 ± 0.26	1.08 ± 0.27	< 0.001[*]

Data are expressed as mean ± standard deviation

ADC, apparent diffusion coefficient; *FROC*, fractional-order calculus; *NMIBC*, non-muscle-invasive bladder cancer; *MIBC*, muscle-invasive bladder cancer

*Indicates statistically significant difference with p value < 0.0125 using Bonferroni-Holm-adjusted significance level
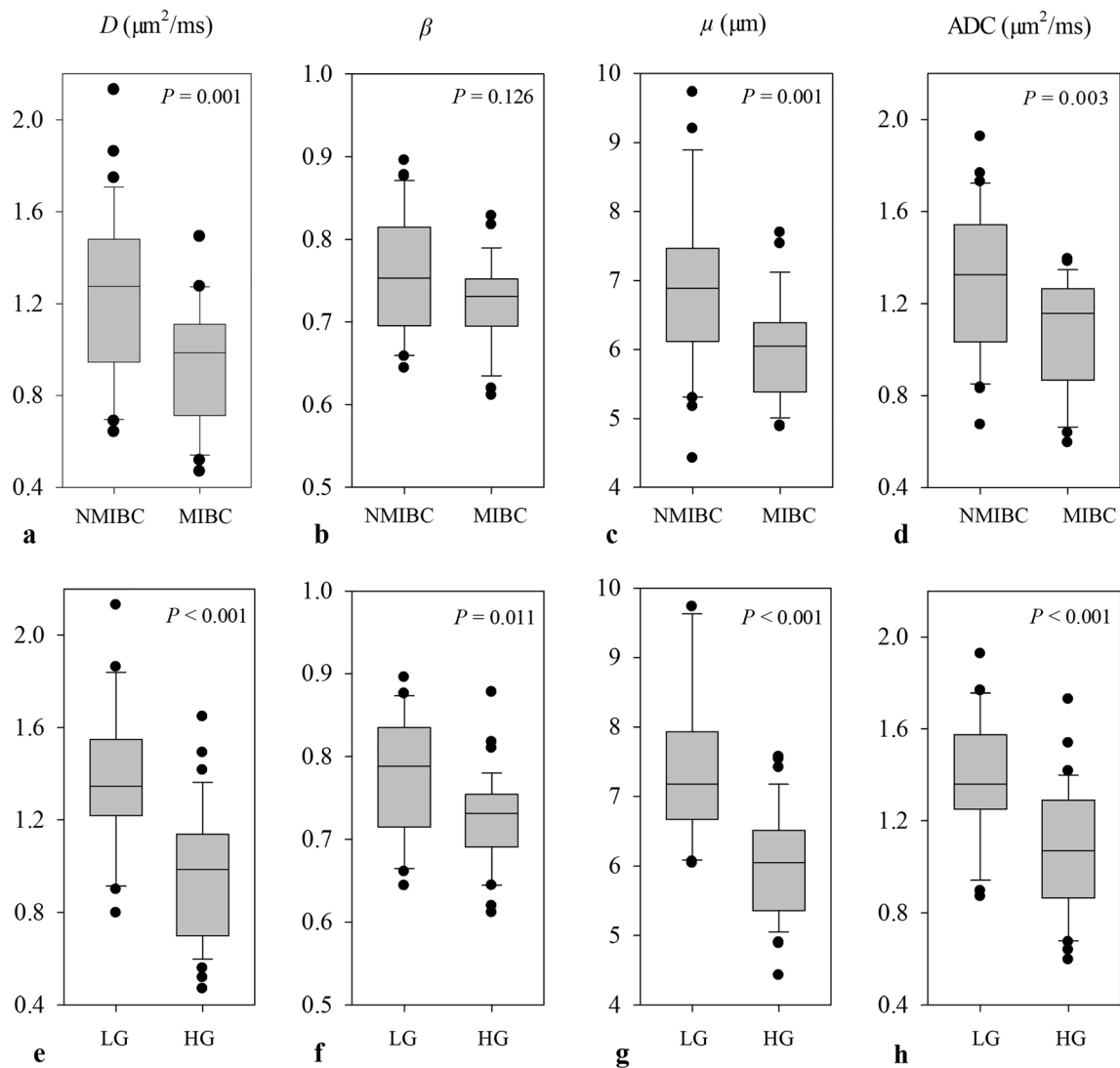
Fig. 4 Box-and-whisker plots showing the comparisons of mean values of the FROC parameters D (**a**, **e**), β (**b**, **f**), and μ (**c**, **g**), and ADC (**d**, **h**) between the NMIBC and MIBC groups (top row), and between the low- and high-grade tumor groups (bottom row). The boxes represent the values from the 25th to the 75th percentiles, whereas the middle line indicates the median value of the individual parameter. The solid dot "●" denotes the outliers that are greater than the 90th percentile, or lower than the 10th percentile. All parameters exhibited significant differences ($p \leq 0.011$) except for β in the upper row

(89%), specificity (86%), and accuracy (88%). Significantly higher sensitivity (89%, $p = 0.031$), accuracy (88%, $p = 0.039$), and AUC (0.892; $p = 0.038$) were observed in the combination (D, β, μ) than in ADC for tumor grading.

For inter-observer reliability of bi-parametric VI-RADS ratings between the two radiologists, a weighted kappa coefficient of 0.846 was achieved, indicating good consistency. The bi-parametric VI-RADS analysis yielded a diagnostic accuracy of 88% and an AUC of 0.859 with a threshold score of 3 or greater for differentiating NMIBC from MIBC. When combined with the FROC parameters (D, β, μ), the performance of bi-parametric VI-RADS increased to 90% in diagnostic accuracy and 0.931 in AUC.

Discussion

We have observed that the FROC parameters D and μ outperformed the conventional ADC in distinguishing low- from high-grade tumors. Moreover, the combination of the FROC parameters (D, β, μ) improved the diagnostic performance over using individual FROC parameters for delineating NMIBC from MIBC and low- from high-grade bladder urothelial carcinomas. Importantly, incorporation of FROC DWI into a simplified version of VI-RADS — bi-parametric VI-RADS — enhanced the diagnostic accuracy of bi-parametric VI-RADS. With these results, our study demonstrated the feasibility of using the FROC diffusion model as a potential non-invasive tool to complement assessments based on histopathology and VI-RADS [12, 13].

Table 3 Diagnostic performance of the FROC parameters (D, β, and μ) and ADC for delineating NMIBC from MIBC and low- from high-grade urothelial carcinoma

Parameter	NMIBC vs. MIBC				Low-grade vs. high-grade			
	Sensitivity (%)	Specificity (%)	Accuracy (%)	AUC	Sensitivity (%)	Specificity (%)	Accuracy (%)	AUC
D	76 (19/25) [63, 86]	69 (23/33) [56, 81]	72 (42/58) [59, 83]	0.755 [0.624, 0.886]	76 (28/37) [62, 86]	86 (18/21) [73, 93]	79 (46/58) [66, 89]	0.842 [0.741, 0.942]
β	76 (19/25) [63, 86]	52 (17/33) [38, 65]	62 (36/58) [48, 74]	0.618 [0.468, 0.768]	78 (29/37) [65, 88]	62 (13/21) [48, 74]	72 (42/58) [59, 83]	0.701 [0.565, 0.838]
μ	84 (21/25) [72, 92]	67 (22/33) [53, 78]	74 (43/58) [61, 85]	0.745 [0.613, 0.878]	78 (29/37) [65, 88]	81 (17/21) [68, 90]	79 (46/58) [66, 89]	0.857 [0.762, 0.952]
Combination (D, β)	68 (17/25) [54, 79]	85 (28/33) [72, 93]	78 (45/58) [64, 87]	0.782 [0.657, 0.907]	84 (31/37) [71, 92]	81 (17/21) [68, 90]	83 (48/58) [70, 91]	0.875 [0.787, 0.964]
Combination (D, μ)	84 (21/25) [72, 92]	67 (22/33) [53, 78]	74 (43/58) [61, 85]	0.752 [0.620, 0.883]	81 (30/37) [68, 90]	81 (17/21) [68, 90]	81 (47/58) [68, 90]	0.870 [0.779, 0.961]
Combination (β, μ)	72 (18/25) [58, 83]	79 (26/33) [66, 88]	76 (44/58) [63, 86]	0.770 [0.642, 0.897]	84 (31/37) [71, 92]	86 (18/21) [73, 93]	84 (49/58) [72, 93]	0.885 [0.801, 0.970]
Combination (D, β, μ)	68 (17/25) [54, 79]	85 (28/33) [72, 93]	78 (45/58) [64, 87]	0.782 [0.657, 0.907]	89 (33/37) [78, 96]	86 (18/21) [73, 93]	88 (51/58) [76, 95]	0.892 [0.810, 0.974]
ADC	72 (18/25) [58, 83]	67 (22/33) [53, 78]	69 (40/58) [55, 80]	0.730 [0.594, 0.865]	73 (27/37) [59, 84]	76 (16/21) [63, 86]	74 (43/58) [61, 85]	0.804 [0.692, 0.916]

Data in brackets are 95% confidence intervals

ADC, apparent diffusion coefficient; *AUC*, area under the receiver operating characteristic curve; *FROC*, fractional-order calculus; *MIBC*, muscle-invasive bladder cancer; *NMIBC*, non-muscle-invasive bladder cancer
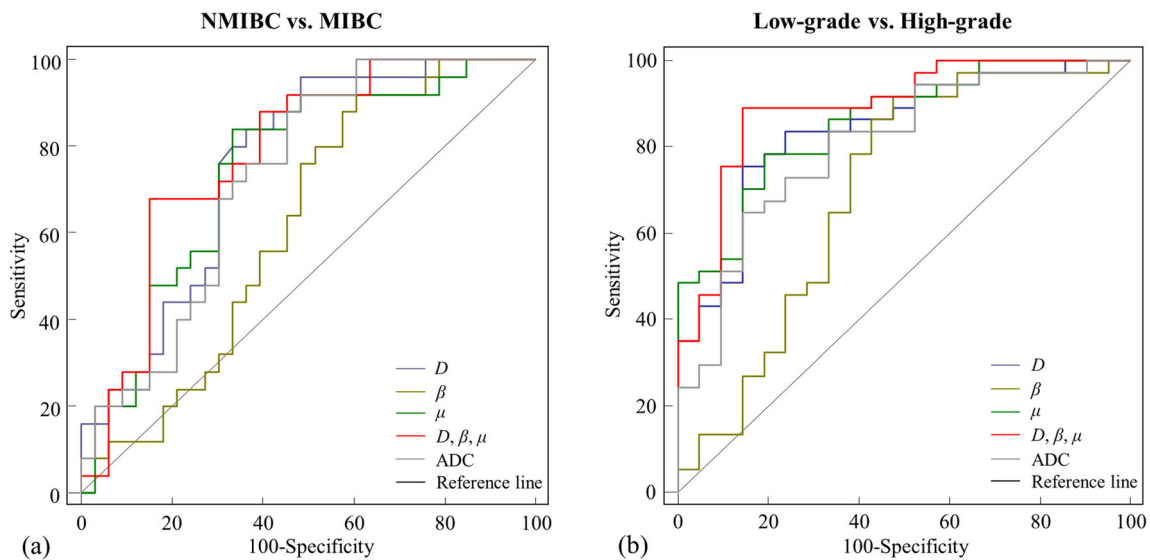

Fig. 5 ROC curves of the individual FROC parameters and the combination of D, β, and μ, together with those from conventional ADC, for differentiating between the NMIBC and MIBC groups (**a**) and between the low- and high-grade tumors (**b**). The combination of D, β, and μ yielded the highest AUCs for distinguishing NMIBC from MIBC (AUC = 0.782) and for tumor grading (AUC = 0.892)

Unlike the mono-exponential diffusion model used for ADC calculation, the FROC model offers three parameters D, β, and μ. Similar to diffusion coefficient in other diffusion models, D in the FROC model is influenced by tumor cellularity, cell membrane integrity, and other structural attributes affecting water diffusion processes in tissues [6, 7, 30]. In our study, the muscle-invasive or high-grade tumors exhibited lower D values than their non-muscle-invasive or low-grade counterparts. This can be associated with the increased cellularity and decreased extracellular space tortuosity that occur in many neoplastic processes [6, 7].

Parameter β has been increasingly related to intravoxel structural heterogeneity [16–18, 20, 31, 32]—an important tissue property that has not been extensively investigated by diffusion imaging. In this study, a reduction in β value was observed in the high-grade tumor group as compared with the low-grade group. This is likely a reflection of a higher degree of heterogeneous clusters of poorly differentiated cells accompanied by vascular hyperplasia, necrosis, and hemorrhage in high-grade urothelial carcinoma [33]. This finding was consistent with other studies on brain tumors [17, 18, 34–36]. Suo et al [37] employed an alternative high b-value non-Gaussian diffusion model—diffusion kurtosis model—to correlate diffusion parameters with the histologic grade of bladder cancer. They observed that a kurtosis-based heterogeneity index, K_{app}, was significantly higher in the high-grade than in the low-grade tumors. Since a lower β value corresponds to a higher degree of tissue heterogeneity [16, 18, 20], our results are consistent with those reported in reference [37]. However, we did not observe a significant change in β between non-muscle-invasive and muscle-invasive urothelial carcinomas, possibly due to the limited sample size. FROC parameter μ has been related to the mean free diffusion length [32]. As such, a strong correlation between μ and D is expected. This correlation was indeed observed in our study both for differentiating NMIBC from MIBC and for differentiating low-from high-grade tumors as shown in Table 2 and Fig. 4. Similar strong correlations between D and μ have also been reported in brain tumor studies [17, 18].

We observed that the specificity for distinguishing NMIBC from MIBC was considerably improved by combing the multiple FROC parameters (D, β, μ), which also provided significantly higher sensitivity, accuracy, and AUC over ADC for tumor grading. The improved diagnostic performance can be attributed to their ability to characterize both diffusion restriction and diffusion heterogeneity. Similar improvements have been reported for characterizing other cancers [18–20].

Recent introduction of VI-RADS provides a systematic way for MRI-based assessment of muscle-invasiveness of bladder cancer [12, 13]. Wang et al [38] reported that VI-RADS score can correlate well with muscle invasion in bladder cancer. The present implementation of VI-RADS includes DWI with at least two b-values from which an ADC map is produced by employing a mono-exponential model. This approach, while simple, does not take advantage of the rich information afforded by high b-value DWI with more sophisticated non-Gaussian diffusion models. Our study has provided preliminary evidence suggesting that the combination of the FROC parameters and VI-RADS can enhance the performance of VI-RADS by simultaneously probing multiple tissue properties including cellularity, heterogeneity, and other aspects of microstructures.

Our study has limitations. First, the distribution of pathologic grades was uneven with more high-grade than low-grade and more NMBIC than MBIC tumors which may bias the statistical analysis. Second, employing a logistic regression algorithm with three predictors (D, β, and μ) is subject to overfitting. The relatively small sample size compromised our ability to perform cross-validation analysis with an independent set of data to mitigate this potential overfitting problem. Third, although TURBT was employed as a reference standard in this study for patients who did not undergo cystectomy, it has its own limitations [4, 5]. Lastly, the present study used only a simplified version of VI-RADS due to the lack of DCE-MRI data. However, the simplified bi-parametric VI-RADS has been reported to yield comparable diagnostic performance to the full VI-RADS analysis [21]. Integration of FROC diffusion imaging into a VI-RADS protocol, using either a bi-parametric or a full multi-parametric approach, will likely lead to further improvement for bladder cancer characterizations, as suggested by our results.

Conclusions

We have demonstrated that the FROC model parameters, individually or conjointly, can be useful for delineating NMIBC from MIBC and low- from high-grade bladder urothelial carcinomas. The FROC model parameters can outperform the conventional ADC and enhance the performance of bi-parametric VI-RADS. With further validation, the FROC diffusion model may become a potential imaging-based tool to aid histopathology and VI-RADS for characterizing bladder urothelial carcinoma.

Declarations

Guarantor   The scientific guarantor of this publication is Cui Feng.

Conflict of interest The authors of this manuscript declare no relationships with any companies whose products or services may be related to the subject matter of the article.

Statistics and biometry One of the authors (M. Muge Karaman) has significant statistical expertise.

Informed consent Written informed consent was obtained from all participants in this study.

Ethical approval Institutional Review Board approval was obtained.

Methodology
• Prospective
• Diagnostic or prognostic study
• Performed at one institution

References

1. Bray F, Ferlay J, Soerjomataram I et al (2018) Global cancer statistics 2018: GLOBOCAN estimates of incidence and mortality worldwide for 36 cancers in 185 countries. CA Cancer J Clin 68:394–424
2. Babjuk M, Burger M, Compérat EM et al (2019) European association of urology guidelines on non-muscle-invasive bladder cancer (TaT1 and carcinoma in situ) - 2019 update. Eur Urol 76:639–657
3. Alfred Witjes J, Lebret T, Compérat EM et al (2017) Updated 2016 EAU guidelines on muscle-invasive and metastatic bladder cancer. Eur Urol 71:462–475
4. Herr HW, Donat SM (2008) Quality control in transurethral resection of bladder tumours. BJU Int 102:1242–1246
5. Ark JT, Keegan KA, Barocas DA et al (2014) Incidence and predictors of understaging in patients with clinical T1 urothelial carcinoma undergoing radical cystectomy. BJU Int 113:894–899
6. Padhani AR, Liu G, Koh DM et al (2009) Diffusion-weighted magnetic resonance imaging as a cancer biomarker: consensus and recommendations. Neoplasia 11:102–125
7. Tang L, Zhou XJ (2019) Diffusion MRI of cancer: from low to high b-values. J Magn Reson Imaging 49:23–40
8. Kobayashi S, Koga F, Kajino K et al (2014) Apparent diffusion coefficient value reflects invasive and proliferative potential of bladder cancer. J Magn Reson Imaging 39:172–178
9. Kobayashi S, Koga F, Yoshida S et al (2011) Diagnostic performance of diffusion-weighted magnetic resonance imaging in bladder cancer: potential utility of apparent diffusion coefficient values as a biomarker to predict clinical aggressiveness. Eur Radiol 21:2178–2186
10. Abou-El-Ghar ME, El-Assmy A, Refaie HF, El-Diasty T (2009) Bladder cancer: diagnosis with diffusion-weighted MR imaging in patients with gross hematuria. Radiology 251:415–421
11. Wang Y, Shen Y, Hu X et al (2020) Application of R2* and apparent diffusion coefficient in estimating tumor grade and T category of bladder cancer. AJR Am J Roentgenol 214:383–389
12. Panebianco V, Narumi Y, Altun E et al (2018) Multiparametric magnetic resonance imaging for bladder cancer: development of VI-RADS (vesical imaging-reporting and data system). Eur Urol 74:294–306
13. Pecoraro M, Takeuchi M, Vargas HA et al (2020) Overview of VI-RADS in bladder cancer. AJR Am J Roentgenol 214:1259–1268
14. Li Z, Li H, Wang S et al (2019) MR-Based radiomics nomogram of cervical cancer in prediction of the lymph-vascular space invasion preoperatively. J Magn Reson Imaging 49:1420–1426
15. Wang F, Chen HG, Zhang RY et al (2019) Diffusion kurtosis imaging to assess correlations with clinicopathologic factors for

16. Zhou XJ, Gao Q, Abdullah O, Magin RL (2010) Studies of anomalous diffusion in the human brain using fractional order calculus. Magn Reson Med 63:562–569
17. Sui Y, Xiong Y, Jiang J et al (2016) Differentiation of low- and high-grade gliomas using high b-value diffusion imaging with a non-Gaussian diffusion model. AJNR Am J Neuroradiol 37:1643–1649
18. Sui Y, Wang H, Liu G et al (2015) Differentiation of low- and high-grade pediatric brain tumors with high b-value diffusion-weighted MR imaging and a fractional order calculus model. Radiology 277:489–496
19. Karaman MM, Tang L, Li Z, et al (2021) In vivo assessment of Lauren classification for gastric adenocarcinoma using diffusion MRI with a fractional order calculus model. Eur Radiol 31:5659-5668
20. Tang L, Sui Y, Zhong Z et al (2018) Non-Gaussian diffusion imaging with a fractional order calculus model to predict response of gastrointestinal stromal tumor to second-line sunitinib therapy. Magn Reson Med 79:1399–1406
21. Pizzi AD, Mastrodicasa D, Marchioni M et al (2021) Bladder cancer: do we need contrast injection for MRI assessment of muscle invasion? A prospective multi-reader VI-RADS approach. Eur Radiol 31:3874–3883
22. Dice LR (1945) Measures of the amount of ecologic association between species. Ecology 26:297–302
23. Menard S (2002) Applied logistic regression analysis. Sage, Thousand Oaks California
24. Perkins NJ, Schisterman EF (2006) The inconsistency of "optimal" cutpoints obtained using two criteria based on the receiver operating characteristic curve. Am J Epidemiol 163:670–675
25. Fagerland MW, Lydersen S, Laake P (2013) The McNemar test for binary matched-pairs data: mid-p and asymptotic are better than exact conditional. BMC Med Res Methodol 13:91
26. Hanley JA, McNeil BJ (1983) A method of comparing the areas under receiver operating characteristic curves derived from the same cases. Radiology 148:839–843
27. Union for International Cancer Control (2017) TNM classification of malignant tumours, 8th edn. Wiley-Blackwell, Hoboken
28. Humphrey PA, Moch H, Cubilla AL et al (2016) The 2016 WHO classification of tumours of the urinary system and male genital organs—part B: prostate and bladder tumours. Eur Urol 70:106–119
29. Liu Y, Zhang Y, Cheng R et al (2019) Radiomics analysis of apparent diffusion coefficient in cervical cancer: a preliminary study on histological grade evaluation. J Magn Reson Imaging 49:280–290
30. Wang Y, Hu D, Yu H et al (2019) Comparison of the diagnostic value of monoexponential, biexponential, and stretched exponential diffusion-weighted MRI in differentiating tumor stage and histological grade of bladder cancer. Acad Radiol 26:239–246
31. Magin RL, Akpa BS, Neuberger T, Webb AG (2011) Fractional order analysis of Sephadex gel structures: NMR measurements reflecting anomalous diffusion. Commun Nonlinear Sci Numer Simul 16:4581–4587
32. Magin RL, Abdullah O, Baleanu D, Zhou XJ (2008) Anomalous diffusion expressed through fractional order differential operators in the Bloch-Torrey equation. J Magn Reson 190:255–270
33. O'Brien T, Cranston D, Fuggle S et al (1995) Different angiogenic pathways characterize superficial and invasive bladder cancer. Cancer Res 55:510–513
34. Karaman MM, Wang H, Sui Y et al (2016) A fractional motion diffusion model for grading pediatric brain tumors. Neuroimage Clin 12:707–714
35. Karaman MM, Sui Y, Wang H et al (2016) Differentiating low- and high-grade pediatric brain tumors using a continuous-time random-

walk diffusion model at high b-values. Magn Reson Med 76:1149–1157

36. Karaman MM, Zhang J, Zhu W et al (2021) Quartile histogram assessment of glioma malignancy using high b-value diffusion MRI with a continuous-time random-walk model. NMR Biomed 34:e4485

37. Suo S, Chen X, Ji X et al (2015) Investigation of the non-gaussian water diffusion properties in bladder cancer using diffusion kurtosis imaging: a preliminary study. J Comput Assist Tomogr 39:281–285

38. Wang H, Luo C, Zhang F et al (2019) Multiparametric MRI for bladder cancer: validation of VI-RADS for the detection of detrusor muscle invasion. Radiology 291:668–674